Journal of Sciences, Islamic Republic of Iran 18(3): 269-284 (2007) http://jsciences.ut.ac.ir
University of Tehran, ISSN 1016-1104

Mineralogy, Geochemistry and Genesis of Titanium Rich Rocks of Qara Aqaj Area, Urmia, Northwest Iran

A. Yaghubpur,[1,*] Y. Rahimsouri,[1,2] and S. Alipour[2]

[1]*Department of Geology, Tarbiat Moalem University, 49 Mofateh Av.,Tehran, Islamic Republic of Iran*
[2]*Department of Geology, Urmia University, km 12 Nazlou Road, Urmia, Islamic Republic of Iran*

Abstract

Qara Aqaj titanium potential is one of the two major known titanium resources in Iran. The main host rocks of the ore body are ultramafics including wehrlite and lherzolite with minor clinopyroxenite. Qara Aqaj intrusion is composed mainly of ultramafic-mafic rocks, layered gabbro, diorite, microdiorite and some monzonite and alkali syenite. This intrusion has intruded the basement complex (amphibolite schist and gneiss), and it is covered unconformably by upper Permian sandstone and limestone. Therefore the age of intrusion can possibly be pre upper Permian. Based on structural and geochemical characteristics, Qara Aqaj intrusion can be divided into basal and main zones. The basal zone is composed of fine grain gabbro with weak layering and alteration, probably originated from a primary tholeiitic magma. This zone is enriched in Si, Na, Mg and Cr and poor in Fe, Ti and P relative to the main zone. Due to low oxygen fugacity ($fO2$) Fe-Ti minerals are not crystallized in the basal zone. It seems that the main zone that forms the main body of the Qara Aqaj intrusion is injected into the tholeiitic magma. Based on the results from drilling four ore bearing wehrlite layers varying in thickness from 1.5 m to 22 m with 33.5 m maximum combined thickness are recognized. Gabbro layers that are in contact with ultramafic layers have no economic mineralization. Some uneconomic oxide minerals are found as inclusions in silicate minerals, or open space fillings. Ore minerals in the ultramafic rocks cropping out in the study area include (in average) 10.58% wt ilmenite, 9.21% wt Ti bearing magnetite, 6.09% wt magnetite and 3.46% wt apatite (fluorapatite). The ore minerals in core samples are as follows (in average): 8.93% wt ilmenite, 8.27% wt Ti bearing magnetite, 5.52% wt magnetite and 4.25% wt apatite. The weight ratio of Fe-Ti oxide minerals to apatite varies from 4 to 30 (average 8). Qara Aqaj titanium potential can be considered as a large titanium bearing orebody. It is similar to the low grade apatite-ilmenite-magnetite deposit in the Kauhajarvi gabbro in western Finland.

Keywords: Titanium; Magmatic ilmenite; Qara Aqaj; Ultramafics; Northwest Iran

Introduction

Qara Aqaj titanium potential is located 37 km northwest of Urmia in the western Azarbaijan province, NW Iran (Fig. 1). This potential has an estimated

[*]*E-mail: yaghubpur1002000@yahoo.com*

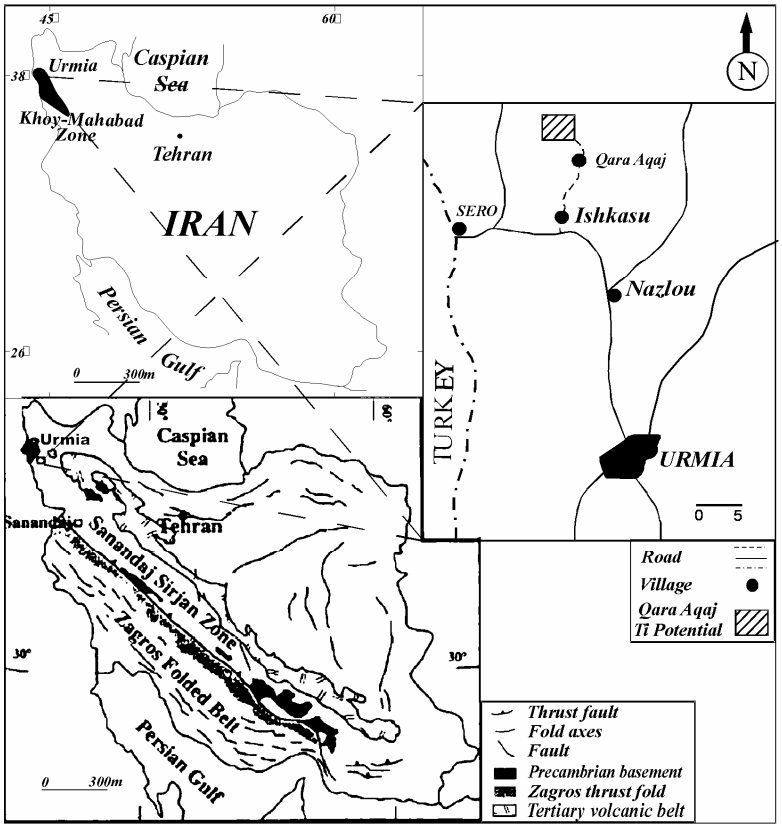

Figure 1. Location map of the Qara Aqaj titanium potential, NW of Iran and its relation to the Khoy-Mahabad zone according to Nabavi [32] and Sanandaj-Sirjan zone according to Stocklin [48].

reserve of about 200 million tones of ore grading 9.32% wt TiO2 in average and 80 million tones of ore grading 4% wt P2O5 [1]. The results of previous investigations reveals the possibility of TiO2 separation in the Qara Aqaj potential [13,18,29,30,39].

Methodology

In this study 291 surface samples, 74 core hole samples, 69 thin and 35 thin polished sections were studied. 152 samples for major oxides including TiO2, Fe2O3, P2O5 and trace elements and 46 samples for the major elements were analysed by XRF. Also 30 samples were analysed for REE by ICP-MS method. The analyses were carried out in China (Wuhan university). Point counter (Basingstoke-James Swift& Son model) were used for volume percent estimation of opaque minerals, apatite (fluorapatite) and silicate minerals. Two G816 magnetomter of 0.1 nanotesla accuracy were used for lateral and depth estimation of the ore body. SEM-EDS analyses were also used to study ilmenite and Ti bearing magnetite.

Geology and Stratigraphy

Qara Aqaj intrusion is an ultramafic (non ophiolitic) Fe-Ti bearing ore body in Iran [39]. It is located in Khoy-Mahabad structural zone according to Nabavi [32] and placed in Sanandaj-Sirjan zone according to Stocklin [48] (Fig. 1). This intrusion is located in the extreme northwest of central Iran zone according to Haghipour *et al.* [10].

Based on the geological map of the studied area, scale 1/20000 (Fig. 2) the regional stratigraphy of the area are presumably as follows:

1. Late Neoproterozoic rocks including gneiss, amphibolite, schist and some marble. The gneiss is also believed to be mylonitized granite and the amphibolite is believed to be mylonitized gabbro and ultramafic rocks (M. Sabzei, written communication).
2. Cambrian sediments that crop out in small extent.
3. Permian sediments including sandstone, limestone, and dolomite in 2000 m (?) thickness, overlying unconformably the Cambrian and older formations [10].

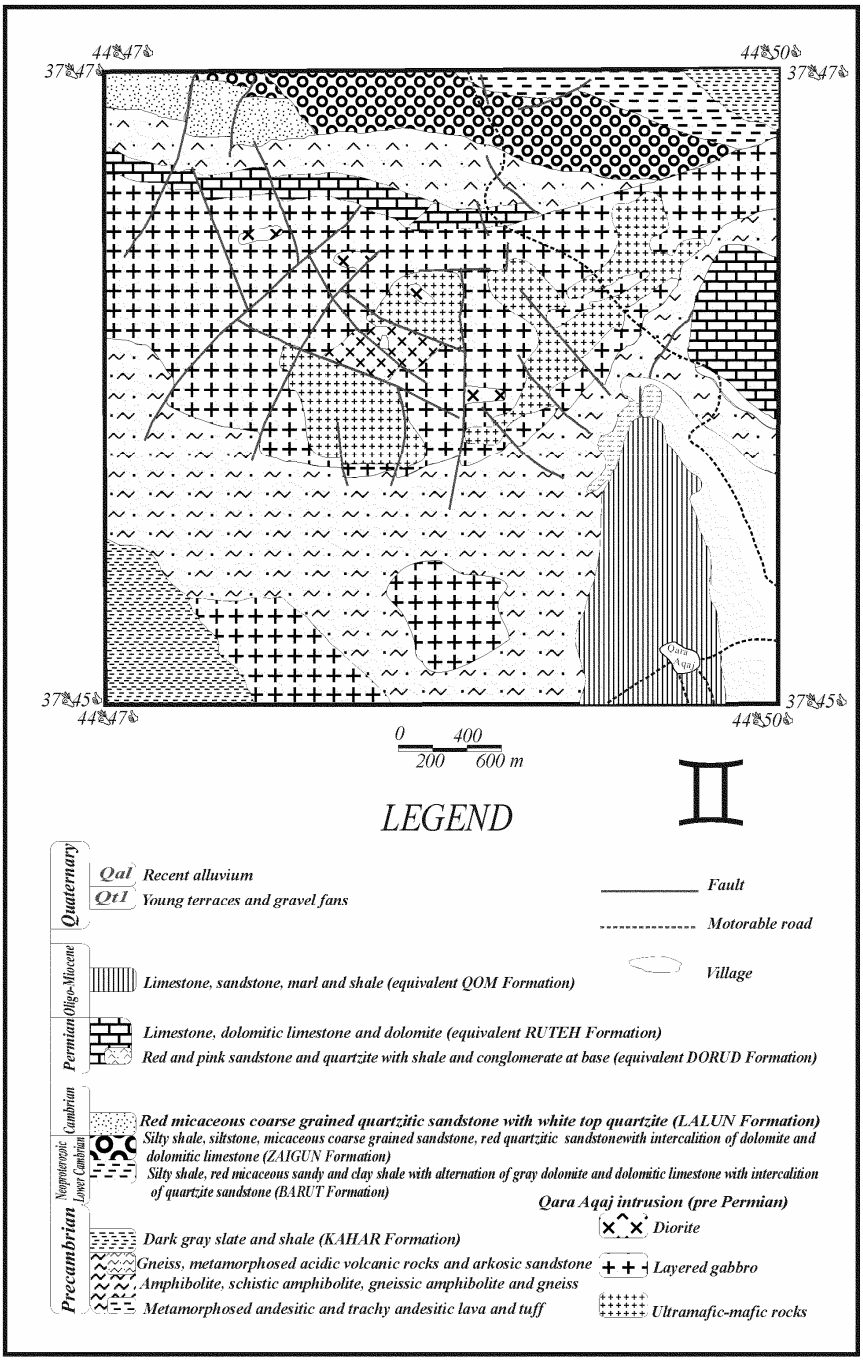

Figure 2. Geological map of the Qara Aqaj titanium bearing intrusion, Urmia, NW Iran [37].

4. Oligo-Miocene sediments including limestone, marl and sandstone, overlied unconformably the older formations.

5. Quaternary sediments including alluvium and young terraces with some travertine.

Qara Aqaj intrusion intruded Precambrian rocks. This body is then overlain by upper Permian sandstone and limestone. Thus the Qara Aqaj intrusion appears to be pre upper Permian in age (M. Sabzei, written communication). The region has experienced many orogenic movements such as Baikalian, Hercynian, Variscan, Caledonian, Cimmerian, Laramian and Pyrenian [46].

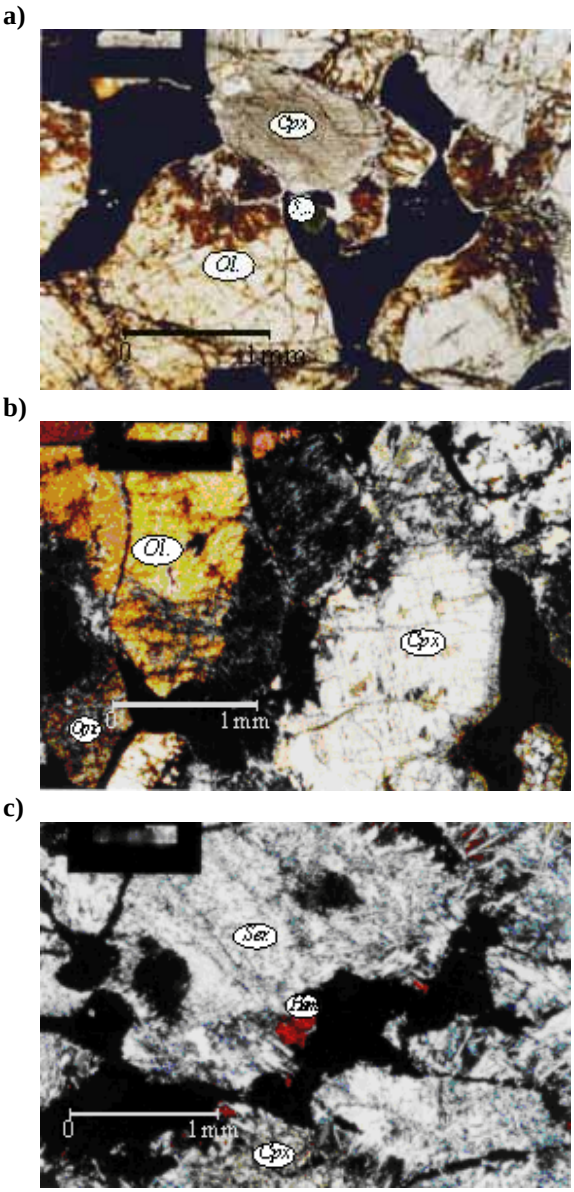

Figure 3. Microphotographs of Fe-Ti oxides and apatite host rocks: **a** Wehrlite, **b** Lherzolite, and **c** Clinopyroxenite in transmitted light. Ol.: Olivine, Cpx.: Clinopyroxene, Opx.: Orthopyroxene, Sp.: Spinel, Ser.: Serpentine, Hem.: Hematite.

Qara Aqaj Intrusion

General Description

The Qara Aqaj intrusion has 4.5 km length, 300 m to 1100 m width. Three systems of faulting have been recognized and were measured in this intrusion: 1) NW-SE trend (N120-140, 50-60 NE) that forms the major faulting system 2) NE-SW trend (N030-040, 65-75 SE) and 3) N-S trend (N160-170, 40-50 E).

The main rock types of the intrusion include wehrlite and lherzolite with some clinopyroxenite. There are 4 mineralized layers enriched in Fe-Ti oxides, ranging in thickness from 1.5 m to 22 m. Changes in thickness can be related to distance from the magma injection site or feeder zone [2,7]. Some of the ultramafic layers not enriched in Fe-Ti oxides, may indicate sporadic liquid immiscibility in magma [45,53]. Parallel layering resembles this potential to concordant type titanium deposits [9,35], that have usually low Fe-Ti oxides and apatite [6].

Wehrlite: Wehrlitic rocks with subhedral granular and cumulate textures, composed of olivine (forsterite), 35-50 vol% (0.15 mm to 1.2 mm), titanaugite and diopsidic augite, 20-35 vol% (0.03 mm to 1.4 mm), opaque minerals up to 18-25 vol%, fluorapatite, 2-9 vol% (0.1 mm to 0.5 mm) and green spinel, 2-9 vol% (0.15 mm to 0.5 mm). Secondary minerals include serpentine, actinolite (±ferroactinolite), chlorite and some anthophyllite (Fig. 3a).

Lherzolite: This rock type with subhedral granular and cumulate texture, composed of olivine (forsterite), 35-50 vol% (0.2 mm to 1 mm), augite and titanaugite 15-25 vol% (0.5 mm to 1.2 mm), hypersthene, 10-15 vol% (0.6 mm to 1 mm), opaque minerals, 20-25 vol%, fluorapatite, 1 vol% to 8 vol% and green spinel, less than 1 vol% associated with secondary minerals such as serpentine, tremolite, actinolite and some talc (Fig. 3b).

Pyroxenite: Clinopyroxenite in small outcrops is present as subhedral granular and cumulate textures, composed of diopside and titanaugite, 75 to 85 vol% and opaque minerals, 20-25 vol% associated with secondary minerals such as tremolite and chlorite with some hematite (Fig. 3c).

Qara Aqaj titanium potential based on host rock petrography, faulting systems and ore grade variations is divided into 11 blocks. Blocks A, B, C and D mainly are hosted by wehrlite, blocks E, F, G, H, I, K and J are hosted by lhrezolite and clinopyroxenite is the host for block D and H (Fig. 4).

Geophysical investigations (magnetometry) indicated the existence of some mineralized ultramafic rocks underlying the layered gabbro. From the results of this investigations and studying the core hole samples the following rock types are recognized: 1) layered gabrro (from surface to 40 m depth), 2) ultramafic-mafic rocks 40 to 102 m depth (with 4 mineralized ultramafic layers), 3) strongly altered gabbroic rocks from depth of 102 to 121.5 m and more (?).

Based on the geochemical characteristics and structural and petrographical studies, Qara Aqaj titanium ore body is divided into main zone (from surface to depth of 102 m) and basal zone (from 102 m down wards).

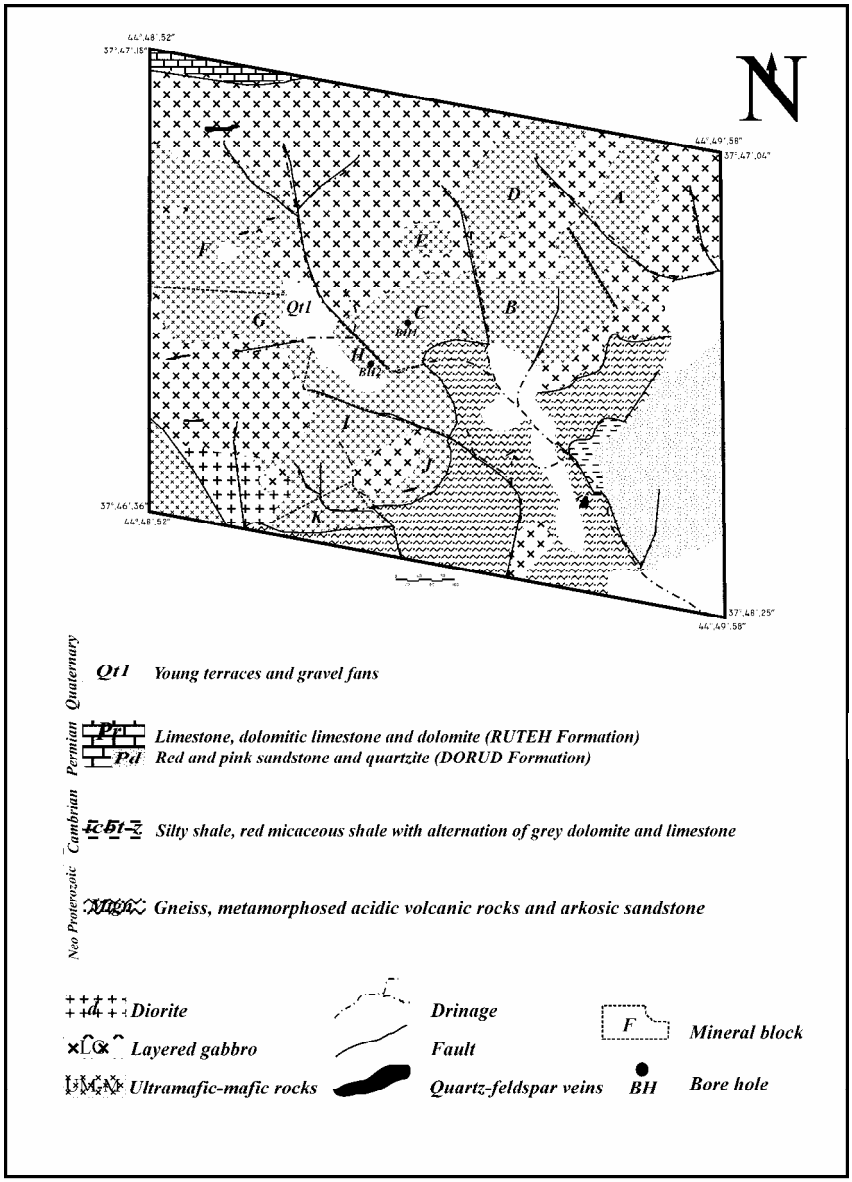

Figure 4. Geological map and mineral blocks of Qara Aqaj titanium potential [37].

Basal Zone: Basal zone is formed of fine grained clinopyroxene gabbro with albitized plagioclase and actinolitized clinopyroxene with some prehnite and calcite that filled the rock fissures. The size of the minerals varies from less than 0.1 mm to 0.4 mm. These rocks are altered to episyenite type rock due to hydrothermal alteration [37]. Opaque minerals include pyrrhotite and some Fe-Ti oxides, that filled mineral spaces. Chemical analysis indicated the amount of TiO2 ranging from 0.68 wt% to 1.07 wt% of the rock. Rocks of the basal zone are subalkaline (Fig. 5a).

Main Zone: Rocks of the main zone are texturally and modally layered, and include 75 vol% of the whole Qara Aqaj intrusion. Four distinct layers from 1.5 m to 22 m in thickness were recognized in this zone. Fe, Ti and P contents of the main zone are high compared to the basal zone, while Cr, Mg, Si and Na are relatively low. Based on AFM diagram, main zone rocks are mainly tholeiitic (Fig. 5b). Chemical analysis (Table 1), normative Ne-Q-Ol (Fig. 5a), AFM diagram (Fig. 5b) and CIPW normative composition (Fig. 5c) indicate a drastic variation between rock types of basal zone compared to the main zone.

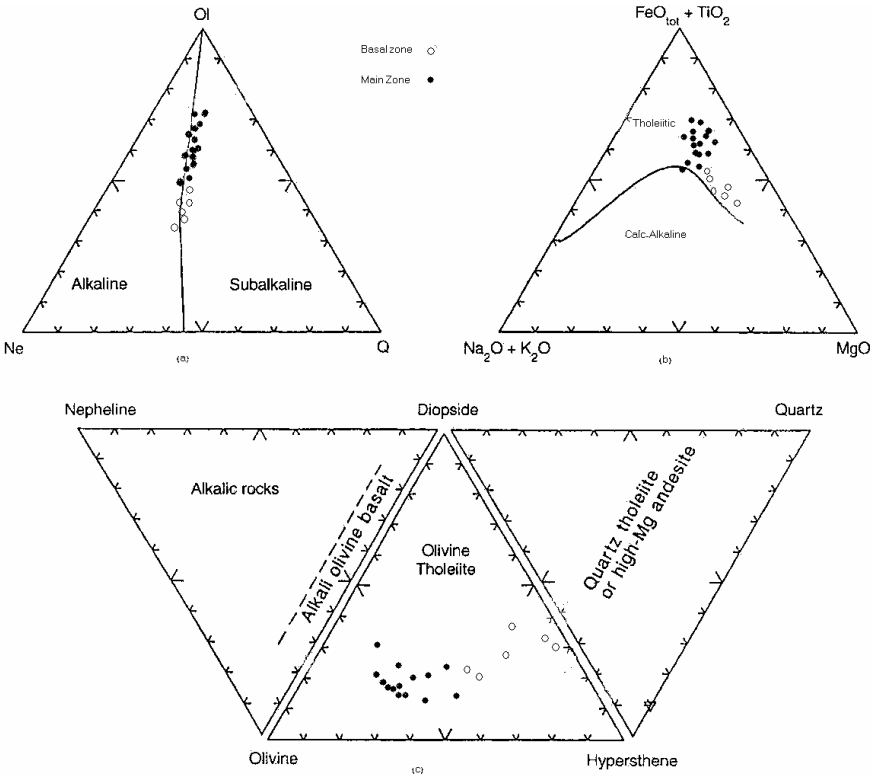

Figure 5. Geochemical classification of basal and main zone rock types, Qara Aqaj intrusion; **a** normative Ne-Q- Ol, **b** AFM diagram, **c** CIPW normative composition . **a** and **b** are according to Irvine and Baragar [14] and **c** in according to Rollinson [43].

Ore Mineralogy

Qara Aqaj intrusion as mentioned earlier can be divided into two zones, and only the main zone contains economical titanium minerals (in ultramafic rocks). Mineralographic studies indicate some opaque minerals such as ilmenite, magnetite, Ti bearing magnetite with minor green spinel, hematite and sulfides including pyrrhotite with minor pyrite [38,40]. Fe-Ti oxide minerals appear in two forms: a) as inclusion with spheroidal texture, hosted by silicate minerals. b) as interstitial (filled the open spaces of intercumulus crystals) and exsolution texture in ilmenite or magnetite. Studied polished and thin polished sections indicated that opaque minerals are apparently formed in separate phases, therefore they bear different textures, grain size and other mineralogical characteristics.

Ilmenite

Three stages in the formation of ilmenite are recognized:

1) As fine inclusion with spheroidal texture [9] with dimensions less than 0.01 mm to 0.2 mm (Fig. 6a). 2) Exsolution texture [41] and lamella (less than 0.01 mm to 0.04 mm) inside magnetite grains (Fig. 6b) that is called ilmenomagnetite [15] and titanomagnetite [41]. 3) As individual, anhedral to subhedral crystals (0.02 mm to 0.8 mm) with granular texture [5], space filling [25] and boundary replacement texture [41] in silicate minerals (Fig. 6c and 6d). Ilmenite contains apatite (fluorapatite), silicates and sulfides as fine inclusions (0.01 mm to 0.06 mm). From economic perspective, the third stage of ilmenites is economic.

Volume and weight percentage of third stage ilmenite were measured in 35 thin polished sections using a point counter based on methods used by Herz and Force [12] and Force [9] (Tables 2 and 3).

Based on weight percentage of apatite and Fe-Ti oxides (Table 3), the ratio of apatite to Fe-Ti oxides in host rocks is between 1:12 to 1:2 in wehrlite, 1:20 to 2:5 in lherzolite and 1:280 to 1:150 in clinopyroxenite. The scatter plots of apatite versus total Fe-Ti oxides do not indicate a nelsonitic trend (Fig. 7).

Weight percentage of economical ilmenite (third stage) and associated minerals in various blocks of Qara Aqaj titanium potential are shown in Table 4.

Table 1. Chemical analysis of basal and main zone rock types [18,37]

Composition	**Basal zone**	**Main zone**		
	Gabbro-Episyenite	*Ultramafic rocks (mainly Wehrlite and Lherzolite)*	*Olivin clinopyroxene gabbro*	*Clinopyroxene gabbro*
SiO2 %	43.17-49.73	22.84-31.13	36.14-41.02	39.89-49.51
TiO2	1.79-2.07	6.40-11.86	3.17-5.88	0.5-2.62
Al2O3	11.97-18.92	4.95-7.62	8.55-14.07	11.76-24.13
FeO(tot)	8.23-11.02	32.02-37.54	18.02-22.43	12.97-17.11
MnO	0.08-0.12	0.38-0.44	0.19-0.35	0.07-0.26
MgO	14.11-18.63	12.04-16.08	8.14-11.07	2.38-7.54
CaO	10.06-12.17	2.79-8.29	5.72-8.11	7.03-10.93
Na2O	3.22-5.98	0.17-0.52	0.77-1.12	1.36-2.57
K2O	0.57-0.74	0.23-0.36	0.56-0.71	0.73-1.02
P2O5	0.62-0.86	0.57-5.05	2.31-4.89	0.20-0.81
S (ppm)	100-1300	81-6849	1226-3006	2393-14118
Ba	56-127	92-349	127-516	91-749
Ni	287-305	62-236	46-112	4-89
Cu	36-171	28-191	39-106	22-76
V	215-402	138-1012	127-571	153-316
Cr	205-392	42-286	56-217	30-177
La	17-51	27-82	15-73	7-64
Ce	10-55	8-65	17-376	12-574
Nd	41-87	34-76	22-62	25-51
Yb	2-3	5-8	3-6	1-6

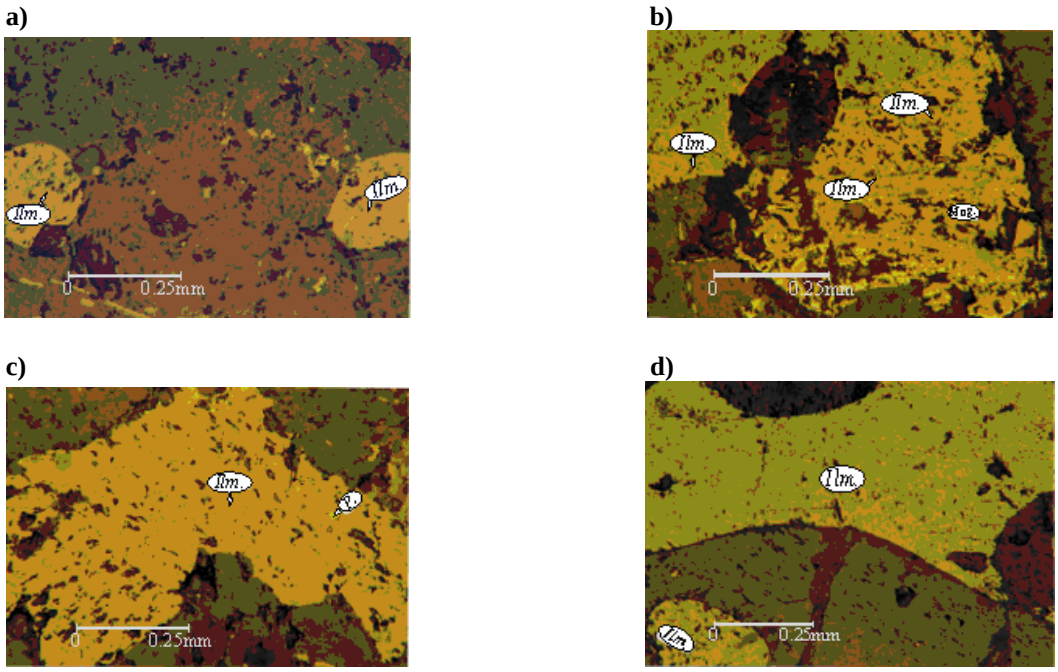

Figure 6. Microphotographs of ilmenite stages of Qara Aqaj titanium potential in reflected light: **a** first stage, **b** second stage, **c** and **d** third stage. Ilm.: Ilmenite, Mag.: Magnetite, P.: Pyrrhotite.

Table 2. Measured volume percent of third stage ilmenite and associated minerals in main zone and basal zone of Qara Aqaj titanium potential by Point counter

Zone	Sample number	Lithology	Ilmenite	Ti bearing magnetite	Magnetite	Hematite	Pyrrhotite	Apatite	Silicates
Main zone									
	A15-44	wehrlite	8.36	8.84	7.39	-	0.75	2.94	71.69
	B6-55	wehrlite	3.89	12.46	8.30	-	0.26	7.93	67.12
	B11-40	wehrlite	5.43	4.16	2.84	-	0.15	7.80	79.59
	B14-37	wehrlite	7.69	5.91	3.97	-	0.35	4.11	77.94
	B23-60	wehrlite	4.04	8.73	13.03	-	0.29	9.03	64.85
	C19-47	wehrlite	10.53	5.35	1.78	-	-	2.21	80.11
	D3-35	wehrlite	9.86	4.41	3.55	-	-	3.56	78.60
	D6-39	clinopyroxenite	12.30	6.59	4.25	0.19	0.36	0.20	76.07
	D17-36	clinopyroxenite	8.91	7.11	4.69	-	-	0.24	79.04
	E5-38	lherzolite	13.08	5.53	4.97	-	0.30	4.32	71.78
	F15-59	lherzolite	11.42	6.51	2.18	-	0.34	1.37	78.15
	F25-34	lherzolite	8.05	6.01	2.93	-	0.29	3.24	79.46
	F16-49	lherzolite	9.18	4.86	3.32	-	0.34	2.15	80.13
	G7-33	lherzolite	8.40	5.58	3.74	-	0.61	7.37	74.28
	G12-42	olivine clinopyroxene gabbro	1.94	6.04	4.09	-	0.25	0.88	86.77
	G30-41	lherzolite	8.14	6.66	4.24	-	-	7.95	73.00
	H6-62	clinopyroxenite	10.40	6.56	5.65	1.05	0.15	0.12	76.04
	H16-66	lherzolite	4.58	10.79	5.35	-	0.90	4.22	74.14
	H28-53	lherzolite	5.28	10.52	7.01	-	0.35	4.53	72.29
	H35-61	clinopyroxenite	12.42	7.35	3.64	0.74	0.31	0.17	75.35
	I1-43	lherzolite	4.33	6.90	4.01	-	-	6.11	78.64
	J12-51	lherzolite	5.23	4.20	2.81	-	0.54	7.92	79.27
	K9-50	lherzolite	5.40	4.31	2.87	-	-	3.54	83.86
	BH1-48	wehrlite	8.16	8.46	6.13	-	0.19	3.60	73.44
	BH2-54	wehrlite	9.83	5.23	3.54	-	2.59	3.43	75.37
	BH3-52	olivine clinopyroxene gabbro	2.05	1.45	1.30	-	0.30	2.55	92.33
	BH4-49	olivine clinopyroxene gabbro	2.61	0.50	0.40	-	1.71	2.30	92.46
	BH6-58	wehrlite	5.54	8.06	5.31	-	0.93	4.37	75.77
	BH7-65	wehrlite	5.31	2.70	1.99	-	0.33	8.13	81.51
	BH8-57	wehrlite	5.08	4.63	2.16	-	1.05	3.96	85.68
Basal zone									
	BH10-67	clinopyroxene gabbro	0.95	2.53	1.05	-	1.63	0.91	92.90
	BH5-63	clinopyroxene gabbro	1.42	2.11	1.64	-	0.47	1.20	93.14
	BH9-64	clinopyroxene gabbro	0.78	1.93	1.10	-	2.81	2.80	90.56
	BH10-56	clinopyroxene gabbro	0.57	0.82	0.62	-	0.38	0.81	96.78
	BH11-45	episyenite	1.04	0.62	0.19	-	4.05	0.52	93.56

Table 3. Measured weight percent of probable economical ilmenite and associated minerals in main zone and basal zone of Qara Aqaj titanium potential

Zone	Sample number	Lithology	Ilmenite	Ti bearing magnetite	Magnetite	Hematite	Pyrrhotite	Apatite	Silicates
Main zone									
	A15-44	wehrlite	10.66	12.23	10.38	-	0.93	2.55	63.22
	B6-55	wehrlite	4.94	17.19	11.63	-	0.32	6.86	59.03
	B11-40	wehrlite	7.38	6.13	4.25	-	0.20	7.21	74.81
	B14-37	wehrlite	10.18	8.49	5.79	-	0.45	3.70	71.37
	B23-60	wehrlite	5.10	11.96	18.14	-	0.35	7.76	56.65
	C19-47	wehrlite	14.00	7.72	2.60	-	-	2.00	73.66
	D3-35	wehrlite	13.08	6.35	5.19	-	-	3.21	72.14
	D6-39	clinopyroxenite	15.88	9.23	6.04	0.27	0.45	0.17	67.92
	D17-36	clinopyroxenite	11.63	10.07	6.74	-	-	0.21	71.33
	E5-38	lherzolite	16.89	7.74	7.07	-	0.38	3.79	64.10
	F15-59	lherzolite	14.98	9.27	3.15	-	0.43	1.22	70.92
	F25-34	lherzolite	10.70	8.66	4.29	-	0.37	2.93	73.03
	F16-49	lherzolite	12.18	7.00	4.85	-	0.44	1.94	73.56
	G7-33	lherzolite	11.11	8.01	5.45	-	0.79	6.64	76.98
	G12-42	olivine clinopyroxene gabbro	2.62	8.87	6.10	-	0.33	0.81	81.25
	G30-41	lherzolite	10.72	9.52	6.15	-	-	7.12	66.48
	H6-62	clinopyroxenite	13.37	9.15	8.01	1.51	0.18	0.10	67.64
	H16-66	lherzolite	5.93	15.16	7.63	-	1.14	3.72	66.40
	H28-53	lherzolite	6.78	14.66	9.92	-	0.44	3.96	64.22
	H35-61	clinopyroxenite	15.97	10.25	5.16	1.06	0.39	0.14	67.00
	I1-43	lherzolite	5.79	10.01	5.91	-	-	5.56	72.72
	J12-51	lherzolite	7.10	6.19	4.20	-	0.71	7.32	74.45
	K9-50	lherzolite	7.33	6.35	4.29	-	-	3.27	78.74
	BH1-48	wehrlite	10.52	11.84	8.71	-	0.24	3.16	65.51
	BH2-54	wehrlite	12.86	7.42	5.10	-	3.31	3.05	68.22
	BH3-52	olivine clinopyroxene gabbro	2.89	2.21	2.01	-	0.41	2.44	90.01
	BH4-49	olivine clinopyroxene gabbro	3.68	0.76	0.62	-	2.36	2.21	90.34
	BH6-58	wehrlite	7.25	11.44	7.65	-	1.19	3.89	68.56
	BH7-65	wehrlite	7.30	4.03	3.01	-	0.44	7.61	77.57
	BH8-57	wehrlite	6.73	6.65	3.15	-	1.36	3.57	78.52
Basal zone									
	BH10-67	clinopyroxene gabbro	1.33	3.85	1.62	-	2.23	0.86	90.08
	BH5-63	clinopyroxen gabbro	1.99	3.21	2.53	-	0.64	1.14	90.46
	BH9-64	clinopyroxene gabbro	1.09	2.93	1.69	-	3.85	2.67	87.75
	BH10-56	clinopyroxene gabbro	0.81	1.27	0.97	-	0.53	0.78	95.62
	BH11-45	episyenite	1.46	0.95	0.29	-	5.58	0.50	91.20

Note: The density of ilmenite, Ti bearing magnetite, magnetite, hematite, pyrrhotite, apatite and silicates (olivine, clinopyroxene and orthopyroxene) are considered 4.07, 5.10, 5.18, 5.26, 4.60, 3.20, and 3.25 in order.

Table 4. Measured weight percentage probable economical ilmenite (third stage), Ti bearing magnetite, magnetite and apatite in various blocks of Qara Aqaj titanium potential

Block	Surface area (m^2)	Host rock	wt% ilmenite	wt% Ti bearing magnetite	wt% magnetite	wt% apatite
A	33023.50	wehrlite	10.66	12.33	10.38	2.55
B	37471.30	wehrlite	6.90	10.94	9.95	6.38
C	34647.70	wehrlite	14.00	7.72	2.60	2.00
D	18051.60	wehrlite	13.08	6.35	5.19	3.21
D	""""""""""	clinopyroxenite	13.75	9.65	6.39	0.19
E	1909.90	lherzolite	16.89	7.74	7.07	3.79
F	69992.30	lherzolite	12.62	8.31	4.09	2.03
G	32419.40	lherzolite	10.91	8.76	5.80	6.88
G	""""""""""	olivine clinopyroxene gabbro	2.66	8.87	6.10	0.81
H	3885.50	lherzolite	6.35	14.91	8.77	3.84
H	""""""""	clinopyroxenite	14.67	9.70	6.58	0.12
I	14530.70	lherzolite	5.79	10.01	5.91	5.56
J	4388.60	lherzolite	7.10	6.19	4.20	7.32
K	4050.60	lherzolite	7.33	6.35	4.29	3.27

Note: The volume ratio of wehrlite to clinopyroxenite in block D and lherzolite to clinopyroxenite in block H is 3 to 1 and the volume ratio of lherzolite to olivine clinopyroxene gabbro in block G is 2 to 1.

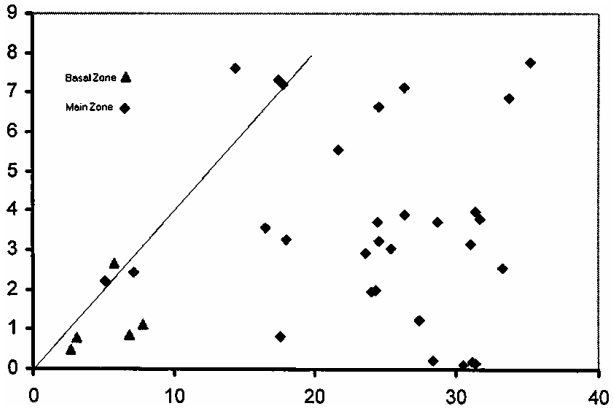

Figure 7. Plot of apatite versus total Fe-Ti oxides; the reference line (apatite versus total oxides: 1:2) is from the ratio of these minerals in nelsonites [36]. Ilmenite,Ti bearing magnetite and magnetite includes separate grains without inclusions and lamella.

The average weight percent of the third stage ilmenite (economical), Ti bearing magnetite, magnetite and apatite in ultramafic mineralized rocks are 10.58, 9.21, 6.09 and 3.46 in surface and 8.93, 8.27, 5.52 and 4.25 in depth ultramafic mineralized rocks respectively. For the Qara Aqaj titanium potential, the ilmenite concentrate contains typically 30 wt% TiO2, that can be recovered by conventional beneficiation [17] and titanomagnetite (second stage ilmenite) concentrate contains typically 4.5 to 6 wt% TiO2 that can be beneficiated by melting method in pilot scale [13]. Semi quantitative analysis of third stage ilmenite and Ti bearing magnetite by SEM-EDS are measured and shown in Table 5 [29,30].

Based on semi quantitative analysis of the third stage ilmenite (Table 5) and the average weight percent of economical ilmenite, TiO2 weight percent of Qara Aqaj titanium potential in surface and at depth are 5.08 and 4.28 respectively. The average TiO2 weight percent mentioned in previous studies by Alipour asl [1] and Kavoshgaran [16] are 9.32 and 8.25, respectively.

Magnetite

Magnetite grains in Qara Aqaj titanium potential consist of 6.09 wt% in surface samples and 5.52 wt% at depth. Magnetite looks to have been formed in four stages: 1) Magnetite as round inclusions (0.05 mm - 0.2 mm) with spheroidal texture inside silicate minerals (Fig. 8a). 2) Magnetite as lamella (less than 0.01 mm to 0.05 mm) with exsolution texture inside the third stage ilmenite (Fig. 8b). 3) Magnetite with granular texture and occasionally replacement and skeletal texture (Fig. 8c). 4) Magnetite showing vein and fracture filling textures [25] from 0.1 mm up to 0.25 mm (Fig. 8d).

Table 5. Semi quantitative analysis of third stage ilmenite and Ti bearing magnetite in Qara Aqaj titanium ore [29,30]

Ore mineral	wt% TiO2	wt% Fe2O3	wt% SiO2	wt% Al2O3	wt% MnO	wt% V2O5	wt% MgO
Ilmenite	48.01	48.33	0.48	0.47	1.14	0.58	0.96
Magnetite	1.23	91.08	1.85	-	0.55	1.46	-

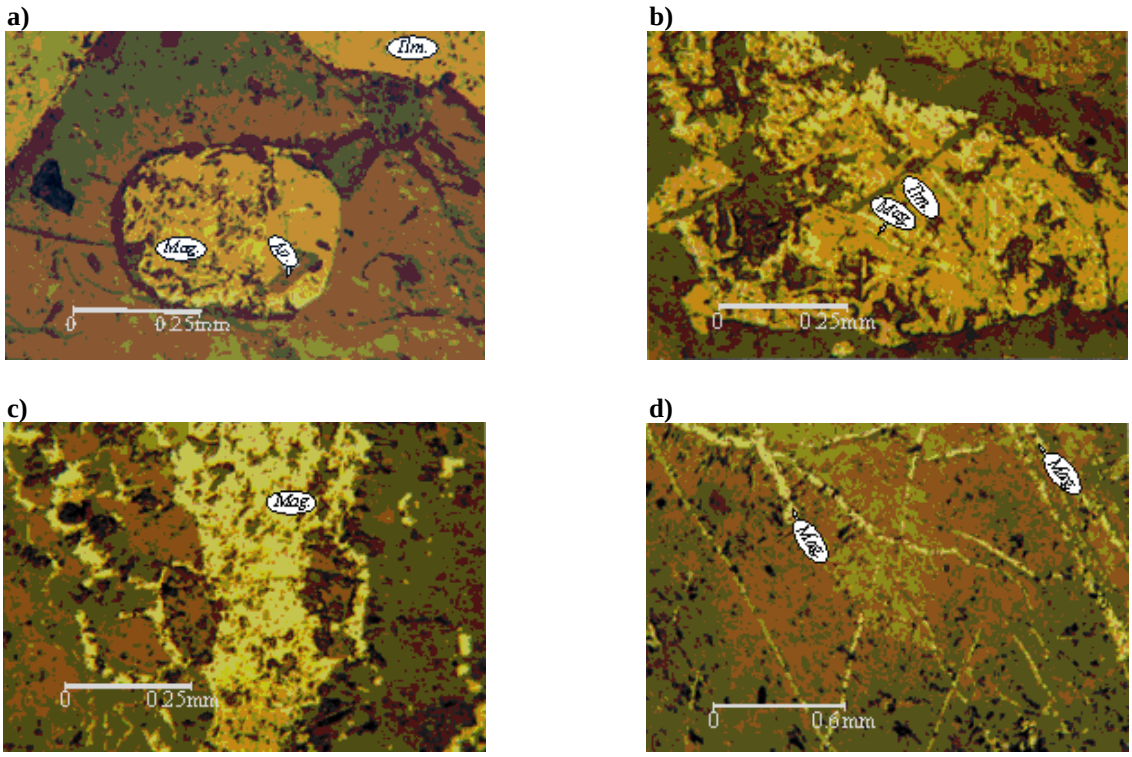

Figure 8. Microphotographs of magnetite stages of Qara Aqaj titanium potential in reflected light: **a** first stage, **b** second stage, **c** third stage and **d** fourth stage. Ilm.: Ilmenite, Mag.: Magnetite, Apa.: Apatite.

Ti Bearing Magnetite

Ti bearing magnetite is formed in one stage with granular and skeletal texture and occasionally appears as veneer form (Fig. 9a, b). Ti bearing magnetite consists 9.21 wt% in surface and 8.27 wt% at depth and the grain size varies from 0.15 mm to 0.7 mm in diameter. It looks to be the result of Ti replacement in magnetite lattice in solid solution state.

Green Spinel

Green spinel seems to have been formed in one stage and mainly has granular texture. Green spinel forms less than 1 wt% of the rocks and range in size from 0.1 mm up to 0.5 mm (Fig. 9c).

Hematite

This mineral with lamellar texture, forms 0.27% wt to 1.51% wt of the rock and is produced by oxidation of magnetite. The size of grains ranges from 0.01 mm up to 0.03 mm and is usually seen in clinopyroxenite host rocks (Fig. 9d).

Sulfide Minerals

Sulfide minerals mainly consist of pyrrhotite and minor pyrite, forming 0.18 wt% to 0.93 wt% in surface and 0.24 wt% to 3.31 wt% in depth of the ultramafic rocks. Rocks in basal zone contain 0.53 wt% to 5.58 wt% sulfide minerals and their sulfide contents are much higher than rocks in the main zone.

Mineralization of pyrrhotite is presumably occurred in 4 stages: 1) Inclusion inside silicate minerals with spheroidal texture (less than 0.01 mm to 0.04 mm), (Fig. 10a). 2) Zonal texture (0.15 mm to 0.25 mm), (Fig. 10b). 3) Minerals with cataclastic texture [25] (0.01 mm up to 0.2 mm), (Fig. 10c). 4) Vein and fracture replacement texture (0.4 mm up to 1.2 mm), (Fig. 10d).

Petrographic Discrimination of Basal and Main Zone by REE

By applying the method used by Karkkainen and Appelqvist [15] for separating the basal zone from main zone of mineralization, in turned out that the average ratio of La/Yb in Qara Aqaj ore body is 12.58 (ranging from 8.5 to 16.66) in the basal zone and 8.03 (ranging from 5.40-10.66) in the main zone. The drastic difference of about 50% in La/Yb ratios can help separating these two zones. This difference also indicates that the main zone can not be differentiated from the residual magma of the basal zone [15].

Discussion and Conclusion

Variations in the amount of ore minerals (Tables 2 and 3), chemical compositions (Table 1), geochemical classification (Fig. 5) and the La/Yb ratio, all are indicative of different magma sources in forming of the basal and main zones.

Slight variation in Fe/Mg ratio in the main zone, high apatite (fluorapatite) and Fe-Ti oxides in this zone indicate that the magma became enriched in Fe, Ti and P, therefore it can be inferred that Qara Aqaj intrusions formed by crystal-liquid fractionation from two magmas.

Due to the abundance of Fe-Ti oxides relative to apatite, a complete nelsonitic trend is not seen but transition from nelsonite to ilmenite-magnetite and apatite rich ultramafic rocks are more visible that has previously been found in other parts of the world [9,22].

The origin of high Fe-Ti bearing anorthosites are explained either by liquid immiscibility [9,12,20,21, 24,34,36,42], or extensive crystallization of plagioclase [28,31,47]. In his studies Watson (1976) showed that in a two melt bimodal system, P and Ti can be enriched. High phosphorous concentrations will increase the titanium solubility in tholeiitic magma [44,49] which finally result to Fe-Ti oxides enrichment in mafic and ultramafic rocks. Therefore it is possible that in Qara Aqaj intrusion the same process has increased Fe and Ti level in these rocks. Fluorine as fluorapatite in the Qara Aqaj tholeiitic magma would probably indicate a crustal origin for these rocks [52].

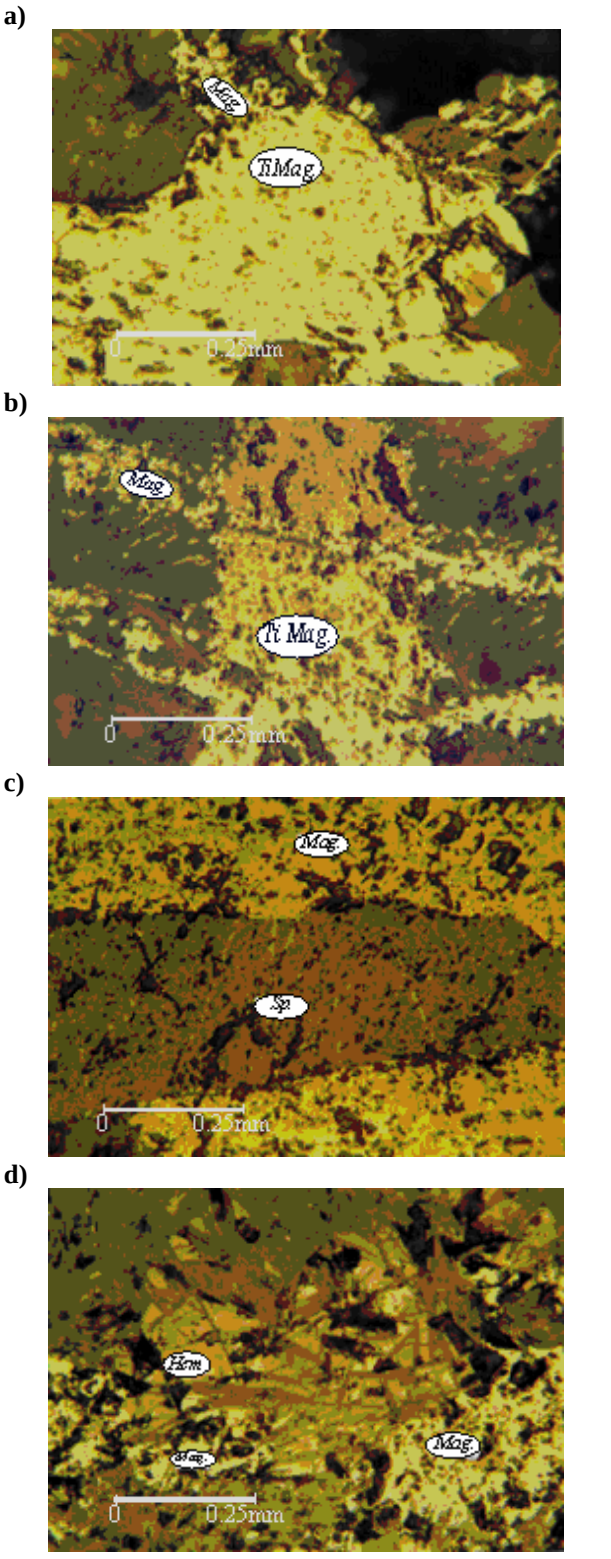

Figure 9. Microphotographs of **a**, **b** Ti bearing magnetite, **c** green spinel and **d** hematite in reflected light, Qara Aqaj titanium potential. Mag.: Magnetite, Ti Mag.: Ti bearing magnetite, Sp.: Spinel, Hem.: Hematite.

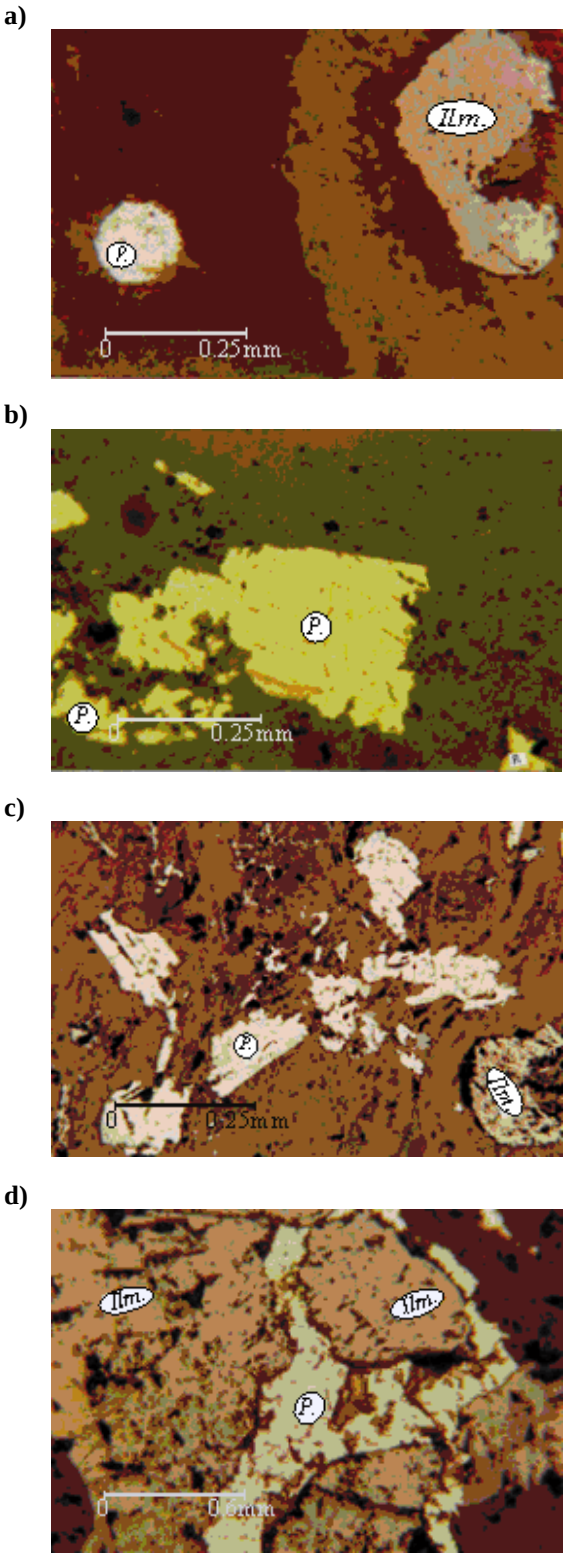

Figure 10. Microphotographs of pyrrhotite stages of Qara Aqaj titanium potential in reflected light: **a** first stage, **b** second stage, **c** third stage and **d** fourth stage. Ilm: ilmenite, P: pyrrhotite.

The basal zone in Kauhajarvi mafic magma (western Finland) is assumed to be relatively non-contaminated mafic magma while the main zone in the Qara Aqaj area indicated to be a contaminated magma [8,15]. This situation can also be the case for Qara Aqaj basal and main zones.

Usually the high oxygen fugacity ($fO2$) and low titanium contents help forming titanomagnetite [3,4,11,19,23,26]. In the main zone of Qara Aqaj ilmenite belongs to the first phase of Ti mineralization (Fig. 6c and 6d) and titanomagnetite is formed in later times (Fig. 6b). Two factors controlling the paragenesis of ilmenite and titanomagnetite (ilmenomagnetite) are high titanium and high phosphorus (more than 1% P2O5) in Fe-Ti rich magma that suppress the crystallization of magnetite relative to ilmenite [50]. In the main zone of Qara Aqaj as Kauhajarvi deposit it seems that apatite was the first mineral to crystallize. This indicates a phosphorus rich magma in Qara Aqaj region, so the high phosphorus concentration caused the crystallization of ilmenite with titanomagnetite (ilmenomagnetite) throughout the main zone [15]. For economic concentrations of Ti and P, the parental magma should have been enriched in these elements [27]. To generate a high grade Ti and P resource by crystal-liquid fractionation, relatively low $fO2$ is required to initially hinder crystallization of Fe-Ti oxides [15,27,33]. In turn, this allows enrichment of titanium relative to iron in the residual magma (as in the basal zone of Kauhajarvi deposit and Qara Aqaj potential) because the ferrous iron is incorporated within olivine and pyroxene minerals [15]. Whereas the conditions of low $fO2$ in the basal zone would favor concentration of titanium in the evolving parent magma, the overall low abundance of titanium in the magma hindered formation of significant mineralized zones in the basal zone as Kauhajarvi deposit. By contrast, the parental magma for the main zone was highly enriched in Ti and P, but the relatively high $fO2$ of this second magma restricted Fe, Ti and P solubility in the crystallizing magma [15]. On the other hand the magma which has produced the main zone had higher $fO2$ and has resulted the formation of 4 low grade layer of titanium mineralization in Qara Aqaj as Kauhajarvi deposit, rather than a single zone of massive Ti and P bearing ore body.

Ore mineral textures, petrographical studies and field relations indicated that the type of titanium mineralization in Qara Aqaj intrusion is magmatic ilmenite and ferrogabbroic facies [9]. According to a model suggesting by Force [9], magmatic ilmenite deposits (based on immiscibility hypothesis) are formed in three stages: 1) Appearance of Fe-Ti oxide droplets

Table 6. Chemical analyses of Ultramafic-mafic rocks in Qara Aqaj potential and Kauhajarvi deposit [15,37]

Mineral resource	**Qara Aqaj titanium potential (Urmia-NW Iran)**		**Kauhajarvi deposit (Western Finland)**	
Lithology	*Peridotite (host rocks)*	*Gabbro*	*Peridotite (host rocks)*	*Gabbro*
SiO2 %	22.84-31.13	39.89-49.51	29.90-33.21	38.39-49.98
TiO2	6.40-11.86	0.5-5.88	5.13-8.24	1.96-4.89
Al2O3	1.95-3.54	11.76-24.13	7.47-8.60	14.20-19.15
Fe2O3	32.02-37.54	5.16-20.71	31.01-35.50	11.99-21.29
MnO	0.38-0.44	0.07-0.26	0.32-0.35	0.17-0.26
MgO	12.04-16.08	2.38-7.54	6.54-9.50	2.42-5.16
CaO	2.79-8.29	7.03-10.93	7.79-8.37	7.41-9.06
Na2O	0.17-0.52	1.36-4.69	0.96-1.35	2.57-4.17
K2O	0.03-0.06	0.23-0.88	0.33-0.49	0.65-1.67
P2O5	<1-5.05	<1-4.89	1.29-2.31	0.63-2.09
S (ppm)	81-6849	2393-14118	1800-4900	100-400
Ba	92-349	91-749	260-340	530-1060
Ni	2-236	4-89	40-67	10-46
Cu	28-191	22-76	70-124	10-48
V	138-1012	153-316	594-830	103-749
Cr	42-286	30-177	12-38	13-76
La	11-78	1-51	13.4-24 .7	9.95-15.0
Ce	2-200	1-124	35.8-61.7	25.1-37.5
Nd	84-104	25-51	26.3-43.6	17.3-26.2
Yb	5-8	1-6	1.85-2.09	1.26-2.11

and precipitation of the droplets to the bottom of cumula. In the study area this stage is texturally represented by spherical inclusions in silicate phases (Fig. 6a and 8a). 2) Formation of concordant cumulate layering in ferrodiorite and related rocks. In Qara Aqaj potential oxides (with or without apatite) are interstitial to cumulate phases and poikilitically enclose them (Figs. 3a-c, 6b, 8b and 9a). 3) Formation of magmatic ilmenite deposits in the form of discordant bodies. The third stage of the model has not been identified yet in Qara Aqaj titanium potential.

On the basis of the host rocks, accompanying rocks, ore mineralogy, structural morphology and chemical composition, one can conclude that the Qara Aqaj titanium potential has several similarities with a low grade apatite-ilmenite-magnetite deposit in the Kauhajarvi gabbro in western Finland, as shown in the Table 6.

Acknowledgements

We would like to thank Professor H. Moinvaziri (emeritus professor-Tarbiat Moalem university of Tehran) for his helps in petrographic investigations. We would also thank Eng. J. Abdullahi sharif (Manager of Kavoshgaran Consultant Engineers-Urmia branch), Eng. M. Hojjati and Eng. A. Taheri (Industries and Mines Organization-Western Azarbaijan) for their financial support. We also like to thank M. Masnabadi for his helps in drafting maps.

References

1. Alipour asl M. Economic geology and petrology of apatite-ilmenite bearing mafic-ultramafic igneous complex in north of Urmia, (NW Iran), M.Sc. *Thesis*, University of Shahid Beheshti, 267 p. (in Farsi) (1996).
2. Arndt N., Jenner G., Ohnenstetter M., Deloule E., and Wilson A.H. Trace elements in the Merensky Reef and adjacent norites Bushveld complex South Africa. *Mineralium Deposita*, **40**: 550-575 (2005).
3. Buddington A.F. and Lindsley D.H. Iron-titanium oxid minerals and synthetic equivalents. *J. Petrol*., **54**: 310-357 (1964).
4. Clark A.H., and Kontak D.J. Fe-Ti-P Oxide melts generated through magma mixing in the Antauta subvolcanic center, Peru: Implications for the origin of nelsonite and iron oxide-dominated hydrothermal deposits. *Econ. Geol.*, **99**: 377-395 (2004).

5. Craig I.R. and Vaughan D.J. *Ore Microscopy and Ore Petrography*. John Wiley Press, 406 p. (1981).
6. Duchesne J.C. Fe-Ti deposit in Rogaland anorthosites (South Norway), geochemical characteristic and problems of interpretation. *Mineralium Deposita*, **34**: 182-198 (1999).
7. Eales H.V. Caveats in defining the magmas parental to the mafic rocks of Bushveld Complex and the manner of their emplacement:review and commentary. *Min. Mag.*, **66**: 815-832 (2002).
8. Emslie R.F. Anorthosite massifs, rapakivi granites, and late proterozoic rifting of North America. *Precam. Research*, **7**: 61- 98 (1978).
9. Force E.R. Geology of titanium-mineral deposits. *USGS* professional paper 259, 112 p. (1991).
10. Haghipour A. and Aghanabati A. *Explanatory Text of the Serow Quadrangle Map 1/250000*. Geological survey of Iran, 58 p. (in Farsi) (1988).
11. Hargraves R.B. Petrology of the Allard lake anorthosite suite. In: Engel A.E. (Ed.), *Petrogenic Studies*, GSA, Buddington Volume, pp. 163-189 (1962).
12. Herz N. and Force E.R. *Geology and Mineral Deposits of Roseland District of Central Virginia*. *USGS* professional paper 1371, 56 p. (1987).
13. Irannejad M. and Montajem M. Beneficiation of Qara Aqaj ilmenite concentrate by melting method. Proceeding of the first Iranian Mining Engineering Conference, pp.849-859 (in Farsi) (2004).
14. Irvine T.N., and Baragar W.R.A. Aguide to chemical classification of the common volcanic rocks. *Can. J. Earth Sci*., **8**: 523-548 (1971).
15. Karkkainen N. and Appelqvist H. Genesis of low grade apatite-ilmenite-magnetite deposit in Kauhajarvi gabbro, western Finland. *Mineralium Deposita*, **34**: 754-769 (1999).
16. Kavoshgaran Consultant Engineers. *Semi detaild exploration report of Qara Aqaj Titan and phosphate Ore*. 203 p. (in Farsi) (1996a).
17. Kavoshgaran Consultant Engineers. *Mineral processing report of Qara Aqaj Titan and phosphate Ore*. 23 p. (in Farsi) (1996b).
18. Kavoshgaran Consultant Engineers. *Detaild exploration (Phase 1) report of Qara Aqaj titanium deposit.* pp. 1- 17 (in Farsi) (1999).
19. Klemm D.D., Henkel J., Dehm R., and Gruenewaldt G. Von. The geochemistry of titanomagnetite in magnetite layers and their host rocks of the eastern Bushveld complex. *Econ. Geol*., **89**: 1075-1088 (1985).
20. Kolker A. Mineralogy and geochemistry of Fe-Ti oxide and apatite (nelsonite) deposits and evaluation of the liquid immiscibility hypothesis. *Ibid.*, **77**: 1146-1158 (1982).
21. Kolker A., Lindsley D.H., and Hanson G.N. Geochemical evolution of the Ranch pluton, Laramie anorthosite complex,Wayoming, trace elements and petrogenetic model. *Am. Minerl.*, **75**: 572-588 (1990).
22. Krause H., Gierth E., and Schott W. Fe-Ti deposits in the south Rogaland igneous complex with special reference to Ana-Sira anorthosite massif. *Norges Geologiske Undersokelse Bulletin* **402**: 25-38 (1986).
23. Lindsley D.H. origin of Fe-Ti deposits in the Laramie anorthosite complex (Abstract). *IGCP* 290 (1991).
24. Lister G.F. The composition and origin of selected iron-titanium deposits. *Econ. Geol*., **61**: 275 -310 (1966).
25. Malekghasemi F. *Principles of Ore Microscopy*. Tabriz University Press, 340 p. (in Farsi) (1999).
26. Mathison C.I. Magnetites and ilmenites in Somerset Dam layered basic intrusion,southeastern Queensland. *Lith*os, **8**: 93-111 (1975).
27. McBirney A.R. The Skaergaaed Intrusion. In: Cawthorn R.G. (Ed.), *Layered Intrusions*, Elsevier, Amesterdam, pp. 147-180 (1996).
28. McLelland J., Ashwal L., and Moore L. Composition and petrogenesis of oxid-,apatite-rich gabbronorites associated with Proterozoic anorthosite massifs: examples from the Adirondack Mountains, New York. *Contrib. Mineral. Petrol*., **116**: 225-238 (1994).
29. Mehdilou A. Mineral processing studies of Qara Aqaj titanium ore with physical methods. *MSc Thesis*, Amir Kabir university. 167 p. (in Farsi) (2003).
30. Mehdilou A. and Irannejad M. Ore dressesing of Qara Aqaj titanium ore. Proceeding of *The First Iranian Mining Engineering Conference*. pp. 1247-1261 (in Farsi) (2004).
31. Mitchell J.N., Scoats J.S., Frost C.D., and Kolker A. The geochemical evolution of anorthosite residual magmas in the Laramie anorthosite complex,Wayoming. *J. Petrol*., **37**: 637-660 (1996).
32. Nabavi M.H. *An Outline to Geology of Iran*. Geological Survey of Iran Press. 109 p. (in Farsi) (1976).
33. Nabil H., Barnes S., and Higgins M. Genesis of phosphorous and titanium deposits in the Spet-Iles mafic intrusion [abs.]: *Canadian Institute of Mining, Metallurgy and Petroleum*, Annual General Meeting, *105th*, Montreal, Programme. pp. 114-115 (2003).
34. Naldrett A.J. Evidence for sulfide and Fe-Ti-P-rich liquid immiscibility in the Duluth Complex, Minnesota. Commentary on the paper by Ripley et al., Economic Geology, V.93: *Society of Economic Geologists Newsletter*, January1999, **36**: p. 5 (1999).
35. Naslund H.R., Aguirre R., Dobbs F.M., Hemriquez F., and Nystrom J.O. The origin, emplacement and eruption ore magmas, IX Congreso Geologico Chileno Actas **2**: 135-139 (2000).
36. Philpotts A.R. Origin of certain iron-titanium oxide and apatite rocks. *Econ. Geol.*, **62**: 203-215 (1967).
37. Rahimsouri Y. Investigation of Qara Aqaj titanium potential, Urmia, West-Azarbaijan province. M.Sc. *Thesis*, Tarbiat Moalem university of Tehran. 156 p. (in Farsi with English abstract) (2001).
38. Rahimsouri Y. and Yaghubpur A. Investigation of Qara Aqaj titanium potential, Urmia. *Proceeding of 21th symposium of geosciences GSI*. pp. 476-478 (in Farsi with English abstract) (2002).
39. Rahimsouri Y., Yaghubpur A., and Moinvaziri H. Investigation of Qara Aqaj titanium potential, NW Iran. *Proceeding of the 8th symposium of Geological Society of Iran*. pp 47-58 (in Farsi) (2004).
40. Rahimsouri Y. and Yaghubpur A. Mineralographic and mineralization studies of Qara Aqaj titanium potential, Urmia (NW Iran). *Proceeding of the 8th symposium of Geological Society of Iran*. p. 790 (in Farsi) (2004).

41. Ramdohr P. *The Ore Minerals and Intergrowth*. 2nd Edition, Pergaman Press. 1174 p. (1980).
42. Ripley E.M., Severson M.J., and Hauck S.A. Evidence for sulfide and Fe-Ti-P-rich liquid immiscibility in the Duluth Complex, Minnesota. *Econ. Geol.*, **93**: 1052-1062 (1998).
43. Rollinson H. *Using Geochemical Data, Evaluation, Presentation, Interpretation.* Longman, John Wiley and Sons, New York (1993).
44. Ryerson F.J. and Hess C. The role of P2O5 in silicate melts. *Geochim. Cosmochim. Acta*, **44**: 611-624 (1980).
45. Sha L.K. Genesis of zoned hydrous ultramafic/mafic-silicic intrusive complexes: an MHFC hypothesis. *Earth Sci. Rev*., **39**: 59-90 (1995).
46. Shahrabi M. *Explanation of Urmia Geological Quadrangle Map*. Geological Survey of Iran Press (in Farsi) (1994).
47. Shaw C.S.J. The petrology of layered gabbro intrusion, eastern gabbro, Coldwell alkaline complex, Northwestern Ontario, Canada: evidence of multiple phases of intrusion in a ring dyke. *Lithos*, **40**: 243-259 (1997).
48. Stocklin J. Structural history and tectonic of Iran, a review. *AAPG Bull*., **K 52**(7): 1229-1258 (1968).
49. Synder D., Carmichael S.E., and Wiebe R.A. Experimental study of liquid evolution in an Fe-rich, layered intrusion: constraints of Fe-Ti oxide precipitation on the T-f O2 and T-P paths of tholeiitic magmas. C*ontrib. Mineral. Petrol*., **113**: 73-86 (1993).
50. Toplis M.J., Libourel G., and Carroll M.R. The role of phosphorus ic crystallization processes of basalts: an experimental study. *Geochim. Cosmochim. Acta*, **58**: 797-810 (1994).
51. Watson E.B. Two-liquid partition coefficients: experimental data and geochemical implications. C*ontrib. Mineral. Petrol*., **56**: 119-134 (1976).
52. Wedepohl K.H. *Handbook of Geochemistry*, V. II/1. Springer, Berlin Heidelberg New York (1970).
53. Zingg A.J. Recrystallization and the origin of layering in the Bushveld complex. *Lithos*, **37**: 15-37 (1996).